Electrospun silk fibroin–gelatin composite tubular matrices as scaffolds for small diameter blood vessel regeneration

Chiara Marcolin[1] ·Lorenza Draghi[1,2] ·MariaCristina Tanzi[2] ·Silvia Faré[1,2]

Abstract In this work an innovative method to obtain natural and biocompatible small diameter tubular structures is proposed. The biocompatibility and good mechanical properties of electrospun silk fibroin tubular matrices (SFts), extensively studied for tissue engineering applications, have been coupled with the excellent cell interaction properties of gelatin. In fact, an innovative non-cytotoxic gelatin gel, crosslinked in mild conditions via a Michael-type addition reaction, has been used to coat SFt matrices and obtain SFt/gel structures (I.D. = 6 mm). SFts/gel exhibited homo-geneous gelatin coating on the electrospun fibrous tubular structure. Circumferential tensile tests performed on SFts/gel showed mechanical properties comparable to those of natural blood vessels in terms of UTS, compliance and viscoelastic behavior. Finally, SFt/gel in vitro cytocompat-ibility was confirmed by the good viability and spread morphology of L929 fibroblasts up to 7 days. These results demonstrated that SFt/gel is a promising off-the-shelf graft for small diameter blood vessel regeneration.

1 Introduction

Because of the increasing incidence of both peripheral arterial occlusive diseases and coronary heart diseases, there is a tremendous need for small diameter vascular grafts [1, 2]. Synthetic grafts (i.e. Dacron®, Goretex®) represent a successful and consolidated solution for the replacement of large and medium diameter vessels (I.D. > 6 mm), but their application as small diameter vessel substitutes presents some limitations such as thrombosis, compliance mis-matches and intimal hyperplasia thus limiting their effec-tiveness in clinics [1–5]. In this regard, the clinical gold standard for small diameter vessel replacement is the use of autologous vessels, such as saphenous vein or internal mammary artery. However, the possible damaged condi-tions of these vessels, due to the presence of cardiovascular

✉ Silvia Faré
silvia.fare@polimi.it

[1] Department of Chemistry, Materials and Chemical Engineering "G. Natta", Politecnico di Milano, Piazza L. Da Vinci 32, Milano, Italy

[2] Local Unit Politecnico di Milano, INSTM, Milano, Italy

This is a post-peer-review, pre-copyedit version of an article published in Journal of Materials Science. Materials in Medicine, 2017, 28:5. The final authenticated version is available online at: http://dx.doi.org/10.1007%2Fs10856-017-5884-9

disease, and the need for repeated surgery procedures limit the use of autologous grafts [6, 7].

To overcome these limitations, vascular tissue engineering represents a promising approach by developing functional grafts with morphological, mechanical and biological properties similar to those of native vessels [8]. In particular, all the limitations encountered by both synthetic and autologous grafts have to be addressed to propose a new strategy for small diameter vascular grafts, where another major requirement is the capability to mimic the natural tissue in terms of structure and function.

The host-material response is mainly related to the kind of the building blocks (i.e., material) and their architecture (i.e., morphology). Concerning the choice of the material, natural polymers are advantageous because of their reduced cytotoxicity and inflammatory host response [9]. In this class, silk fibroin (SF) and gelatin have been shown promising as scaffolding materials [10–13]. In particular, silk from silkworm Bombyx mori has been widely studied and characterized for biomedical applications [14–16]. Bombyx mori silk fibers are composed by two proteins, fibroin and sericin; as sericin can cause possible non-physiological inflammatory reaction, it is necessary its removal by a degumming process. SF after degumming maintains good mechanical properties, biocompatibility, slow in vivo degradation rate, and versatile processability [3]. SF can be processed by different techniques [17–20], where electrospinning (ES) is of particular interest because it allows the production of fibrous structures which can provide a nanofibrous biomimetic architecture for cells. Furthermore, electrospun matrices have a high surface to volume ratio, that offers a large surface area for cell attachment [21]. Finally, ES is a versatile and simple fabrication method, and also tubular scaffolds with desirable diameters may be produced [1, 2, 22]. ES-SF tubes have shown mechanical and biological properties very promising for their possible application as vascular grafts [1, 7, 23]. In fact, their compliance value is close to physiological values reported for Goretex® and Dacron® [2, 24, 25], and the burst pressure of the electrospun SF tubes is higher than in vivo systolic pressure up to pathological values (220 mmHg), even if it is still lower than the typical value of human saphenous vein (1600 mmHg) [26]. Recently, Enomoto et al.[27] demonstrated that a small caliber graft woven from silk fibroin shows in vivo long-term patency and the SF matrix results colonized by endothelial cells and smooth muscle cells. Cattaneo et al. [10] reported the formation of new vascular tissue, with elastin layer in the inner lumen, at 7 days after implantation into rat abdominal aorta.

To further improve the mechanical and biocompatibility properties of SF structures, Marelli et al. [9] proposed an innovative vascular graft by hybridization of electrospun SF tubes with collagen gel. The obtained structure demonstrated compliance value similar to the one of saphenous vein, and good in vitro cell interaction. However, collagen is potentially immunogenic because of its animal origin, and it presents high costs [11]. To overcome these limitations, gelatin can be used as an alternative. Gelatin is a natural polymer obtained from denaturation and partial hydrolysis of collagen [12]; it represents an excellent and promising material for biomedical applications, as it is biocompatible, biodegradable, non-immunogenic, easy to process and inexpensive. Furthermore, gelatin does not activate or bind to platelets [28], which is an important characteristic for a material envisioned for vascular tissue engineering applications. Gelatin gels are currently studied as sealant for vascular prostheses [29] and in many drug delivery systems and tissue engineering applications [13, 30]. However, these gels present two important limitations: the inherent weakness and their solubility at physiological pH and temperature [11]. For this reason, thermal and mechanical stability of gelatin hydrogels has to be improved by physical or chemical crosslinking. Physical methods (e.g. UV-irradiation and dehydrothermal treatment) present some limitations, such as the low efficiency and the difficulty of control the crosslink density. On the contrary, gelatin hydrogels obtained by chemical crosslinking show higher thermal and mechanical stability [13, 29]. However, the crosslinkers (e.g. glutaraldehyde) may induce cytotoxic effects or immunological responses from the host [31]. The combined use of SF and gelatin has been proposed to join the advantages of the two materials and minimize their drawbacks [32–35]. In particular, blends of the two natural polymers have been electrospun to produce scaffolds for vascular tissue engineering or drug delivery systems. Even if preliminary results are promising, this approach has some intrinsic limitations, as crosslinking reaction with 1-ethyl-3-(3-dimethylaminopropyl) carbodiimide (EDC) post-electrospinning results in fiber morphology alteration [33] or in inadequate thermal stability [34].

In the present work, an innovative chemical reaction to crosslink gelatin onto the SF tubular surface is reported. This method occurs in mild conditions and has already proven to allow the production of cytocompatible gels with thermal stability at 37 °C [36]. Crosslinked gelatin gel is used as coating of ES-SF tubular matrices (I.D. = 6 mm) to obtain an innovative small diameter vascular graft. The gel coating is promising to enhance cell interaction and also offers the possibility to be loaded with drugs or growth factors for promoting new tissue formation.

2 Materials and methods

2.1 Materials

Silk fibroin (SF) films were kindly supplied by INNOVHUB —SSI, Div. Stazione Sperimentale per la Seta, Milan, Italy.

Poly(ethylene oxide) (PEO) with a nominal molecular weight of 2×10^5 Da, gelatin type A from porcine skin, triethylamine (TEA), methylenebisacrylamide (MBA), and all basic chemicals were obtained from Sigma Aldrich (Germany).

In vitro cell tests were performed with L929 murine fibroblast cell line (ECACC n° 85011425). Dulbecco's Modified Eagle Medium (DMEM), fetal bovine serum (FBS), dimethyl sulfoxide (DMSO), MTT assay and Alamar Blue® assay were purchased from Sigma Aldrich.

2.2 Electrospun SF tubular matrices (SFts)

Electrospun silk fibroin tubular matrices (SFts, internal diameter, I.D. = 6 mm, length = 20 cm) were obtained from silk fibroin films as previously described [2]. Briefly, SF films were dissolved in formic acid (≈98%) at room temperature under mild stirring at a concentration of 7.5% w/v. Then fibroin solution was perfused by a syringe-pump in an electrospinning equipment. SFts were produced using as collector a stainless steel rotating mandrel (Ø = 6 mm, 2000 rpm) and moving the spinneret along the tube axis (spinneret speed = 140 mm/s) [2].

For an easier removal of the electrospun SFts from the mandrel, a solution of PEO in distilled water (7.5% w/v) was prepared and electrospun on the tubular collector before SF electrospinning. The process parameters used for the two polymeric solutions were 1.1 ml/h flow rate, 10 cm electrode distance, 24 kV voltage and the deposition time was 5 and 180 min for PEO and SF solutions, respectively.

After SF nanofiber deposition, complete solvent evaporation from tubular matrices was achieved by overnight drying at room temperature. Tubes were treated with methanol (>99.9%) for 15 min to induce SF crystallization [2] and PEO was then removed by washing the tubular structures in distilled water at 37 °C under mild stirring for 48 h; at the end, tubular matrices were dried under hood at room temperature till complete water evaporation.

2.3 Electrospun SFts/gelatin composite matrices (SFts/gel)

Electrospun SF tubes were coated with a gelatin gel crosslinked via a Michael-type addition reaction. The gel was prepared by dissolving 1 g of type A gelatin in 6 ml of distilled water at 50 °C; then, 20 µl of TEA were added to increase the pH up to 10 to facilitate the deprotonation of lysine amino groups, that in this way can bind to the crosslinking agent (MBA) methylene groups by breaking the double bond. Finally, MBA was added to the reaction mixture, under stirring. For the crosslinking reaction to occur, the reaction solution has to remain at 50 °C for 24 h [36].

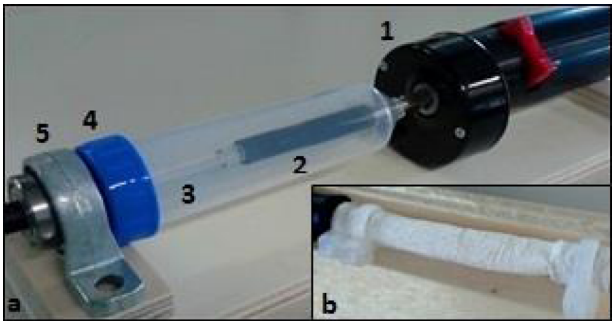

1: rotating battery motor
2: polymeric connections
3: glass rotating mandrel for SFt
4: Falcon tube
5: ball bearing

Fig. 1 SFts coating device. **a** System developed for the gelatin gel coating: the glass mandrel is inserted in the Falcon tube and coupled with a DC motor rotating at 5 rpm. **b** SF electrospun tube mounted on the glass mandrel

In order to achieve a homogeneous coating on the SF tubular structure, it was necessary to maintain SFt structures in mechanical rotation during the gelatin crosslinking. For this purpose, a home-made system was designed and fabricated (Fig. 1a). SFt samples (length = 4 cm) were mounted on a rotating glass mandrel (Fig. 1b) and dipped in gelatin/MBA water solution. The mandrel was then mounted inside a 50 ml Falcon tube and coupled with a motor rotating at 5 rpm. All the components of the system were pre-heated at 50 °C, and the coating was carried out in an oven at 50 °C so to avoid gelatin gelification due to a decrease in temperature before the SFt coating procedure. The system (Fig. 1) was maintained in the oven in order to allow the crosslinking reaction (50 °C, 24 h).

SFt/gel structures thus obtained were purified to eliminate possible unreacted MBA by a washing process, consisting of consecutive steps in pure ethanol and distilled water [36]. The samples were then dehydrated by dipping in ethanol solutions and stored at room temperature under reduced pressure.

2.4 Morphological characterization

The wall thickness of SFt and SFt/gel samples ($n = 7$) after swelling in water was measured with a micrometer (Somet).

The morphology of electrospun fibers was evaluated by scanning electron microscopy (SEM, StereoScan 360, Cambridge Instruments). The average fiber diameter was calculated from SEM images acquired on five different SFt samples. For each sample, 20 measurements were acquired

by using ImageJ v.1.42q software (US National Institute of Health, Bethesda, Maryland, USA, http://rsb.info.nih.gov/ij/).

The distribution of the gelatin coating on SFts was evaluated by SEM analysis. SFt/gel samples were prepared through dehydration of the samples in two concentrations of ethanol solutions (50% for 2 h, and 100% for 2 h). Samples were dried under hood at room temperature, sputter-coated with gold (Edwards Sputter Coater 5150B) and observed with a 10 kV accelerating voltage at different magnifications (500x, 1500x, 5000x).

2.5 Swelling and weight loss analysis

The water absorption and the kinetics of degradation of the gelatin coating were determined by swelling SFt/gel samples in 2 mL distilled water at 37 °C. SFt samples were used as control. Five samples (cylinders, length = 5 mm) for each material were used. Wet sample weight at different time-points up to 25 days was determined by blotting the sample surface with filter paper to remove the water in excess and then weighed immediately. The percentage of water absorption or weight loss of the samples was calculated as follows:

$$\text{Weight variation} = \frac{w_i - w_o}{w_o} \times 100\%, \quad (1)$$

where w_i represents the wet weight of the samples at the time point i and w_0 is the initial dry weight of the samples.

2.6 Mechanical characterization

The mechanical characterization of SFt/gel structures was performed using a dynamic-mechanical analyzer (DMA, Q800, TA Instruments) with tension film grips modified ad hoc. The tubular structure was cut into 5 mm length to prepare o-ring-shaped specimens. The samples ($n = 5$ for each test and material) were soaked in distilled water for 10 min before testing and hooked by two stainless steel L-shaped wrenches (0.5 mm diameter, Fig. 2). The obtained results were compared with the ones of SFt. The following tensile tests were performed at 37 °C: circumferential, cyclic, stress relaxation and recovery.

2.6.1 Circumferential tensile tests

Circumferential tensile tests were performed with a preload of 0.005 N and a force ramp of 0.5 N/min up to sample break. The results are reported as stress/strain curves. Mechanical parameters for both the structures were calculated: elastic modulus (E), ultimate tensile stress (σ_b) and strain at break (ε_b).

In accordance with Catto et al. [1], theoretical burst pressure (P_b) values of the two structures were calculated by rearranging the Laplace's law for a pressurized thin-walled hollow cylinder:

$$P_b = \frac{S \times \sigma_b}{r}, \quad (2)$$

where r and S represent the internal radius of the sample and the wall thickness, respectively.

Fig. 2 Set-up used for mechanical tests; detail of the modified tension film grips

2.6.2 Cyclic tests and calculation of compliance

For cyclic uniaxial tensile tests, samples were subjected to a preload of 0.05 N prior to undergoing 50 cycles of loading/unloading between 0.3 and 0.6 N at a frequency of 1 Hz.

The applied load values were defined upon the transmural pressures that act on a thin wall deformable tubular structure [37, 38]. In fact, the ring-shaped samples were considered as sections of a vessel with homogeneous internal pressure; the circumferential stress σ applied to the wall can be considered homogeneous and calculated again according to Laplace's law (3):

$$\sigma = \frac{r \times P}{S} \quad (3)$$

where P is the pressure across the wall, r and S represent the internal radius of the sample and the wall thickness, respectively. Being σ related to the force (F) applied to the tubular sample of thickness S and length L by (4):

$$F = 2 \times S \times L \times \sigma \tag{4}$$

it is possible to relate the transmural pressure P to F. In particular, force values used during the test correspond to physiological pressure values of 80 and 140 mmHg. The results, in terms of elongation in time, were used to calculate the theoretical values of compliance for the two structures in accordance with the standard ISO/TC 150/SC 2/WG 3 N42:

$$\text{Compliance} = \frac{\frac{\Delta r}{r_1} \times 100}{\frac{\Delta P}{100}}, \tag{5}$$

with $\Delta r = r_2 - r_1$, where r_2 and r_1 are the sample radius dimensions corresponding to the pressure values P_2 and P_1 (140 and 80 mmHg), and $\Delta P = P_2 - P_1$.

2.6.3 Viscoelastic behavior

For stress relaxation analysis, samples were subjected to four cycles of relaxation and recovery. The duration of both the stress relaxation and the recovery phases was 2 min. The strain value applied was set to 10% according to previous work [37] and, as in previous procedures, preload was 0.05 N. The applied strain value belongs to the elastic range of σ/ε curves of the two structures.

2.7 In vitro cell tests

For cell experiment, flat circular samples (Ø = 6 mm) were punched from SFt and SFt/gel conduits, and disinfected with 70% ethanol solution for 1 h and by UV exposure for 15 min. Five disks for each material were seeded with 200 µl of L929 cell suspension (cell density = 10^4 cells/sample) in complete DMEM. Tissue culture polystyrene (TCPS) wells seeded with cells were used as control. After 1, 3 and 7 days, cell viability was evaluated by Alamar Blue® assay by reading the absorbance values at 570 nm using a spectrophotometer (TECAN, Genios Plus). For each time point, cell morphology was analyzed by SEM on samples fixed with 1.5% v/v glutaraldehyde in 0.1 M sodium cacodylate, dehydrated in a graded ethanol series and sputter-coated with gold (Edwards Sputter Coater 5150B).

2.8 Statistical analysis

Data, where applicable, were expressed as mean ± standard deviation and statistically compared by two-tailed t-Test ($n = 5$, significance level = 0.05).

3 Results

3.1 Morphological characterization

3.1.1 SFt structures

Tubular silk fibroin structures with 6 mm internal diameter were successfully obtained by electrospinning process (Fig. 3). The wall thickness of SFt was 212 ± 43 µm. SEM analysis showed homogeneous electrospun fibers (Fig. 3b) with random distribution despite the relatively high rotation speed of the mandrel (2000 rpm). Diameter values of the fibers were in the range 400–1200 nm following a bell-shaped distribution, with curve peak at about 650–700 nm (Fig. 3c).

3.1.2 SFt/gel structures

The coating of SFts with crosslinked gelatin gel (Fig. 4a) caused, as expected, an increase of the wall thickness. In fact, wall thickness of hydrated SFts/gel was 307 ± 45 µm, showing an increase about 44% compared to the SFt one.

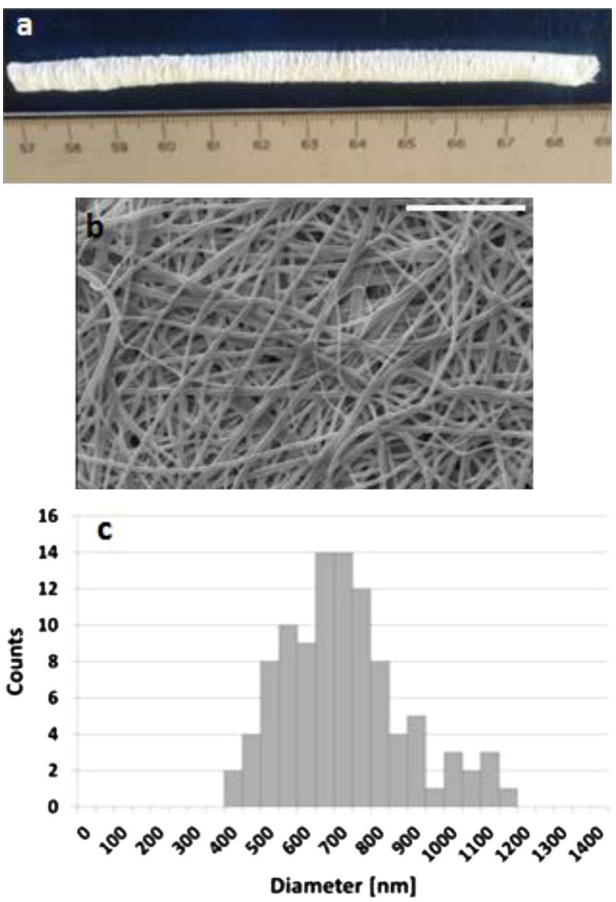

Fig. 3 **a** Macrograph of the electrospun SFt; **b** SEM image of the random distribution of SFt fibers (scale bar = 20 µm); **c** fiber diameter distribution of SFt obtained by ImageJ

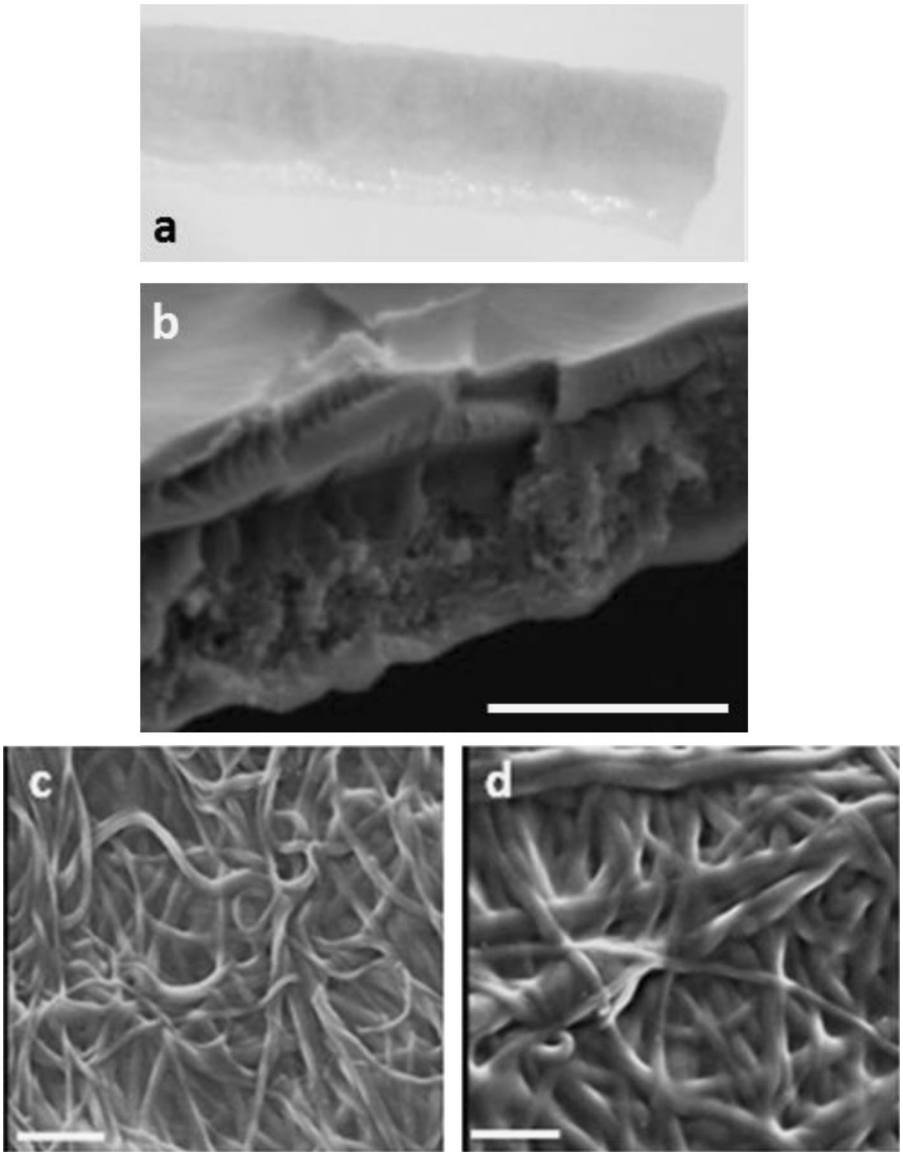

Fig. 4 Morphological characterization of SFt/gel. **a** Macrograph of an as made SFt/gel sample. SEM micrographs of the cross-section **b** (*scale bar* = 20 μm), the external **c** and the internal **d** surfaces of SFt/gel: crosslinked gelatin gel is homogenous on both sides and fiber morphology is still visible (*scale bar* = 10 μm)

The gel reached the internal surface of the tubular structure, without causing occlusion of the tubular sample lumen.

SEM images were used to evaluate the distribution of gelatin gel on tubular samples both on the internal and the external walls of the structure. Figure 4c of the external surface of a SFt/gel sample showed the presence of gelatin coating with a homogeneous distribution on an electrospun matrix whose fibrous structure was still visible. Gelatin was extensively present also on the internal surface of the tubular construct (Fig. 4d), suggesting the homogeneity of coating within the wall thickness of the tube, as shown also in the cross-section of SFt/gel samples (Fig. 4b).

3.2 Swelling and weight loss test

The stability of the gelatin coating was evaluated in water at 37 °C up to 25 days. SFt samples, used as control, reached the plateau in few days (about 50 h), with a mean weight variation of 1100% (Fig. 5).

SFt/gel samples showed greater water absorption with mean weight variation values up to 1600%. The significant difference between SFt and SFt/gel (+45%) is due to the presence of the gelatin gel that has a high ability to swell in water [36]. SFt/gel behavior showed that gelatin coating is stable up to 300 h (about 13 days), then gel degradation occurred, with a slow rate.

3.3 Mechanical characterization

3.3.1 Circumferential tensile tests

The mechanical behavior of SFt and SFt/gel was assessed by circumferential tensile tests. Representative stress-strain curves of the two materials are reported in Fig. 6.

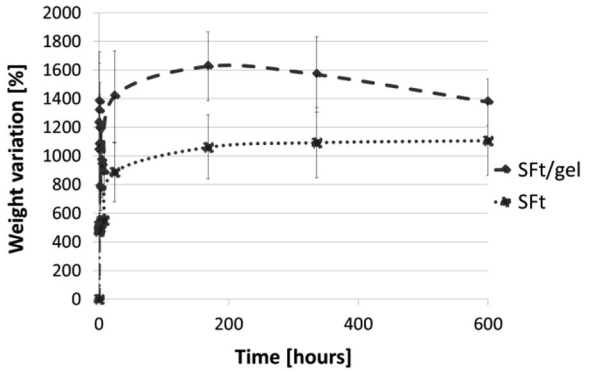

Fig. 5 Swelling behavior and weight loss for SFt and SFt/gel up to day 25 (600 h)

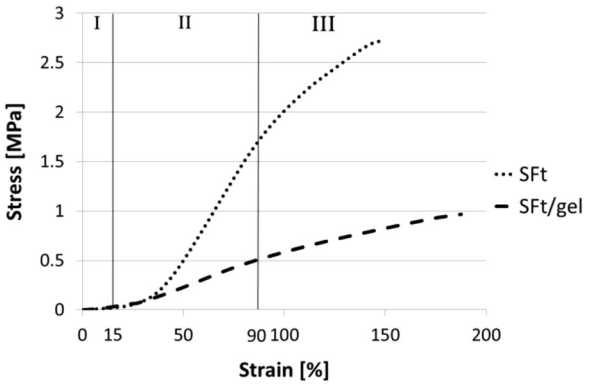

Fig. 6 Representative stress–strain curves for SFt and SFt/gel obtained in circumferential tensile tests

The burst pressure (BP) of the two structures was calculated according with the Laplace's law from the UTS values obtained in the tensile circumferential tests. Even if the burst pressure is higher for SFt (1279 ± 317 mmHg) compared to SFt/gel (1075 ± 444 mmHg), these values are not statistically different ($p = 0.17$, Fig. 7).

3.3.2 Cyclic tests

The results of cyclic tests, in terms of elongation in time, have been used to calculate the compliance between 80 and 140 mmHg for the two structures. SFt/gel has a similar compliance value than SFt (5.48 ± 0.13 and 4.59 ± 0.10 respectively, $p = 0.19$).

3.3.3 Viscoelastic behavior

The representative stress relaxation/recovery behavior of SFt and SFt/gel is illustrated in Fig. 8. Trends showed the typical viscoelastic response, but due to the lower stiffness, SFt/gel structures reached lower stress values than SFt (see Table 1).

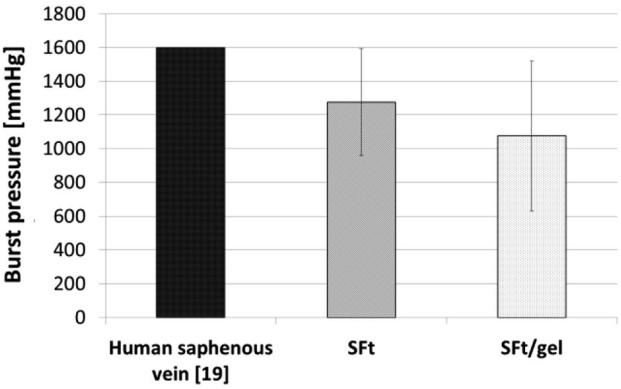

Fig. 7 Estimated burst pressure values of SFt and SFt/gel compared to that of human saphenous vein

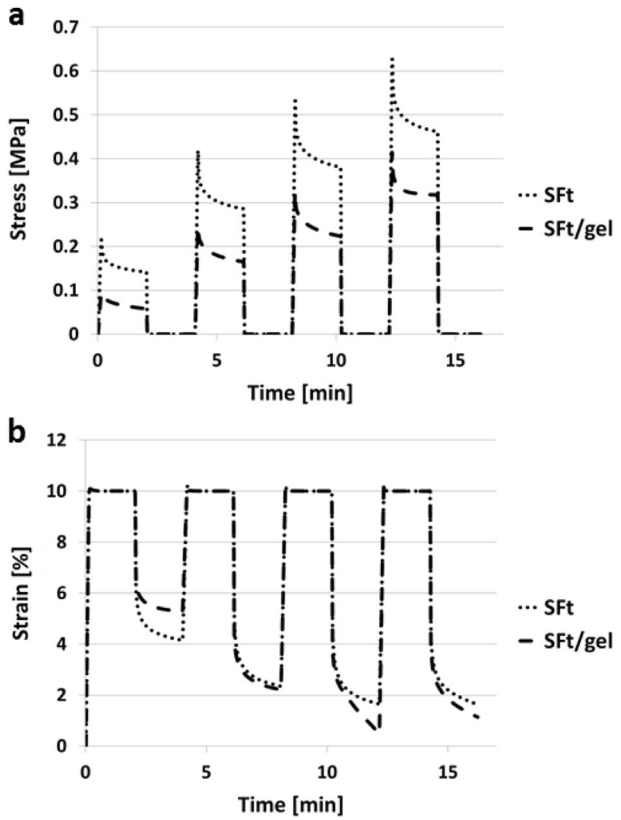

Fig. 8 Stress relaxation **a** and recovery **b** curves of SFt and SFt/gel

3.4 In vitro cell tests

Alamar Blue® assay on cells cultured on SFt and SFt/gel samples revealed a linear increase of L929 cell viability with culture time for both materials (Fig. 9a). In general, there was no statistical difference in cell metabolic activity on the two structures ($p = 0.36$) and, at day 7, cell viability on SFt and SFt/gel was comparable ($p = 0.51$) to control (TCPS).

Table 1 Values of the considered mechanical parameters obtained by circumferential tensile tests for SFt and SFt/gel scaffolds

	Elastic modulus [MPa] (*)	Strain at break (%)	UTS [MPa] (*)	Stiffness region II [MPa] (*)	Stiffness region III [MPa] (*)
SFt	1.82 ± 0.49	141.53 ± 24.40	2.41 ± 0.69	3.01 ± 0.73	1.56 ± 0.19
SFt/gel	0.58 ± 0.25	152.72 ± 41.73	1.17 ± 0.48	0.88 ± 0.30	0.70 ± 0.23

Values are expressed as mean and standard deviation

(*) $= p < 0.05$

SEM micrographs showed L929 cells well adhered to SFt and SFt/gel fibers already 24 h after seeding (Fig. 9b and e). For increasing culture time (i.e., day 3 and day 7), a more flattening and spreading cell morphology was observed (Fig. 9c, f and d, g). 7 days after seeding, the surface of SFt/gel structures was almost entirely covered by flattened fibroblasts, and above them numerous rounded cells were also found probably due to an intense cell proliferation.

4 Discussion

Concerning the morphological characterization, the random nanofiber orientation and morphology obtained has been previously demonstrated to be adequate for the regeneration of small caliber blood vessels in vivo [10]. The diameter of fibers measured is consistent with those reported in previous works [1, 2] for ES-SF tubular structure obtained with the same SF solution concentration and process parameters. Therefore, SF electrospinning proves once again to be a very reproducible process.

The observed swelling behavior for SFts is due to the porous structure of the electrospun matrix, which therefore is able to hold water among the nanofibrous mesh. Results of swelling and weight loss tests for SFt/gel samples proved that the crosslinking method used for gelatin has a positive effect on gel stability, especially if compared to gelatin gels crosslinked with standard methods, i.e. genipin and EDC, which generally are stable up to few days [39, 40]. Such a good stability is an important feature for the application envisioned; in fact, gelatin coating offers both a high cytocompatible substrate, promoting cell adhesion and proliferation, and causes a low platelet adhesion, which are key factors particularly in the early stages of vascular regeneration.

Regarding the mechanical characterization, for each stress-strain curve reported in Fig. 6, three regions have been defined: region I, where low stress values cause high deformations, probably due to the fiber rearrangement towards the direction of the external force applied; region II, with an almost linear response, and region III where a decrease of the slope of the curve for the yielding of nanofibers is observed until break. In particular, although the region I is qualitative similar for SFt and SFt/gel, in region II a higher increase in the stress values (i.e. a higher stiffness, $p = 0.038$) is evidenced for SFt compared to the gelatin coated one. In region III, SFt/gel behavior is slightly different compared to region II; in fact, there is no statistical difference between the stiffness values of the last two regions ($p > 0.073$), whereas for SFt the curve slope decreases significantly compared to region II ($p = 0.042$). Comparing SFt with SFt/gel samples (Table 1), the values of elastic modulus and UTS were significantly different ($p = 0.045$ and $p = 0.042$, respectively). In fact, SFt/gel has lower mechanical properties than SFt due to the presence of gelatin coating, which balances the higher mechanical properties of SF alone. Ultimate tensile stress (UTS) value for SFt confirms the results found by Soffer et al. [22] for SF electrospun tubular structures. Concerning SFt/gel matrices, as expected, the UTS value is higher than those obtained for other natural polymer vascular grafts [41, 42], but lower than synthetic polymer grafts [43, 44] also when coated with collagen [45]. Hence, SF confirms to have excellent mechanical properties among natural polymers. Moreover, UTS value for SFt/gel is very close to that of native aorta (UTS = 1.2 MPa) [43]. SFt/gel elastic modulus is similar to that obtained for ES-SF tubular matrices with smaller diameter (i.e. 1.5 mm) [1], which have been suc-cessfully implanted in rat abdominal aorta [10]. As for UTS value, SFt/gel elastic modulus is higher than that found for natural grafts [42], but lower than synthetic grafts [46]; furthermore, it is in the range of the stiffness of natural blood vessels (E = 0.26–14.5 MPa) [47, 48].

The estimated burst pressure values of the two structures are lower than the burst pressure of the human saphenous vein, considered the gold standard for vascular bypasses; anyway they are much higher than physiological and pathological hemodynamic pressures, so potentially SFt and SFt/gel are able to resist to in vivo stresses caused by blood flow even in pathological condition. Furthermore, after implantation, the graft is intended to be colonized and remodeled by surrounding cells, hence helping it to sustain physiological loading. The estimated BP value for SFt is higher than those reported in other works for ES-SF tubular matrices [1, 2, 9, 22]. This difference can be explained not only by the different method used, but also by the wall thickness which is greater for SFt (ca. 210 μm) compared to

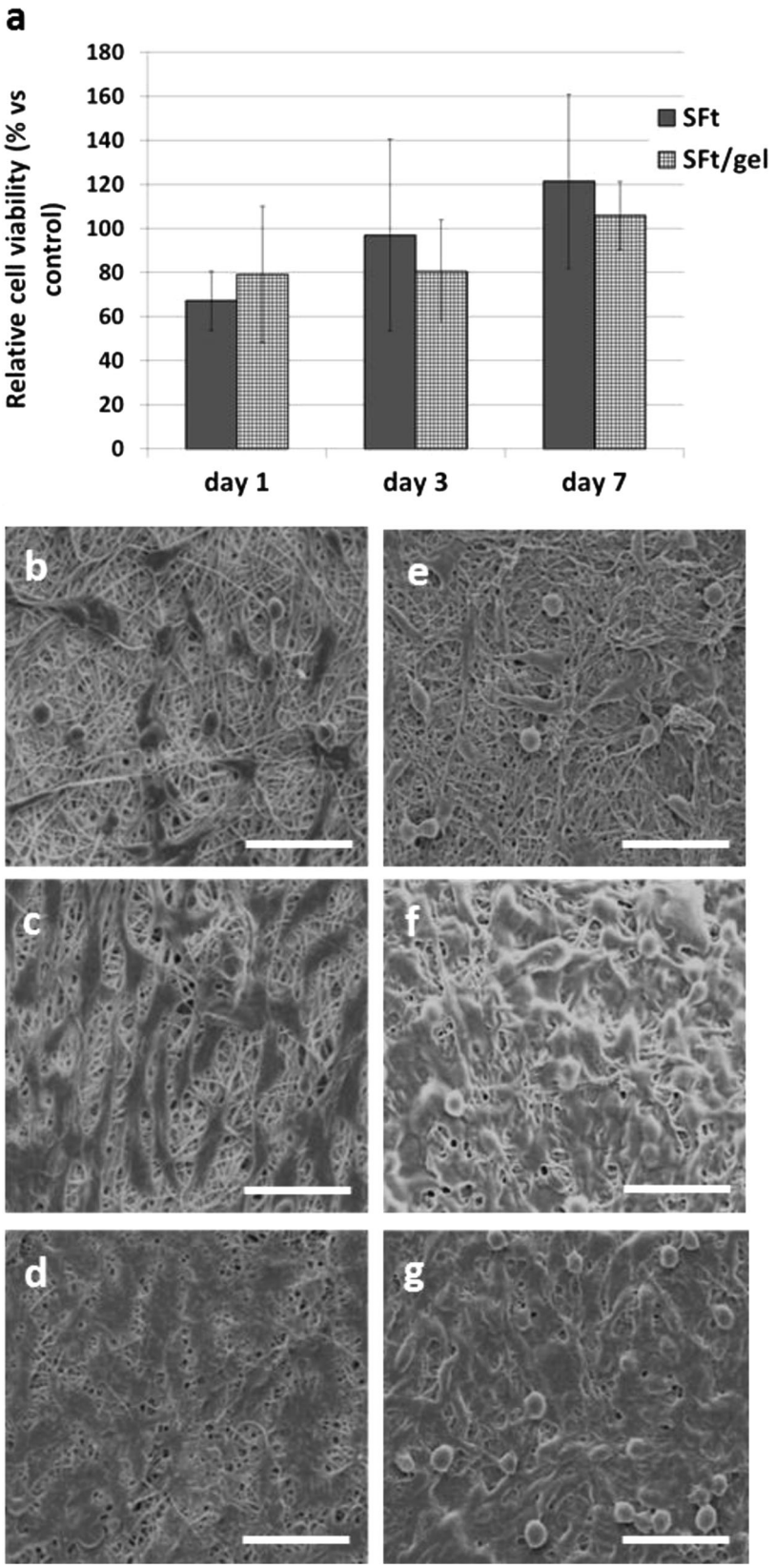

Fig. 9 Biocompatibility characterization of SFt and SFt/gel. **a** Alamar Blue assay showed good cytocompatibility of the two structures, when compared to the control (TCPS). In fact, fibroblasts viability increases with culture time. SEM micrographs of fibroblasts cultured on SFt **b–d** and SFt/gel **e–g** samples at day 1, 3 and 7 respectively. Cells were found spread and flatten out already after 1 day of culture. At day 7, there is a greater number of cells on SFt/gel compared to SFt. *Scale bar* = 50 µm, micrographs taken at 10 kV

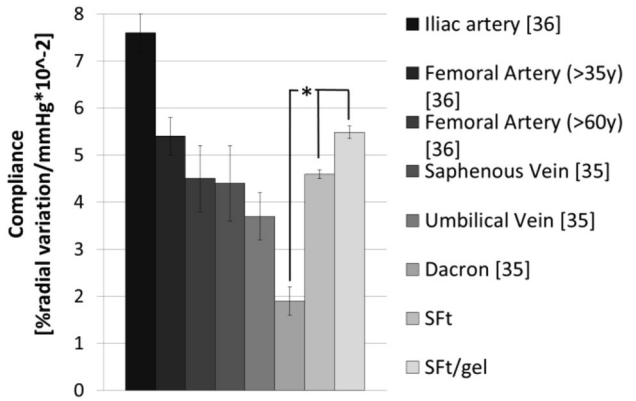

Fig. 10 Estimated compliance values of SFt and SFt/gel compared to those of natural vessels and synthetic material (i.e. Dacron®) used as vascular grafts. (*) = $p < 0.05$

the structures characterized in literature (ca 150–180 μm). SFt/gel structures showed a BP value lower than synthetic grafts [49–53], but higher than other vascular grafts made of natural polymers, such as recombinant tropoelastin electrospun tubular matrices [42] and ES-SF tubes coated with collagen gel [9].

SFt compliance value is similar to that obtained by pre-vious experimental measurements on ES-SF tubular structure [2]. SFt/gel compliance is similar to the experimental one found by Marelli et al. [9] for ES-SF tubes coated with collagen gel. SFt/gel structures showed compliance values close to those of autografts and higher than both synthetic vascular prostheses (i.e. ePTFE, PET) used for vascular replacement and synthetic grafts studied in literature [52](Fig. 10). Therefore, SFt/gel demonstrated appropriate mechanical properties in terms of mechanical strength and elasticity for application as small diameter blood vessel graft.

Finally, stress relaxation and recovery behavior suggests that when SFt/gel undergoes deformation in vivo, its structure will be subjected to a lower stress relaxation then the uncoated one. Peak stress values reached by the two materials were found to increase by increasing the number of cycles. At the end of the first recovery phase, residual deformation (Fig. 8b) is observed as fibers do not have enough time to recover their initial conformation and remain partially aligned. Therefore, during the following cycles, as fibers are partially aligned along the loading direction, deformation requires higher forces. Deformation imposed in subsequent cycles stretches aligned fibers, whose mechanical response is more elastic, causing the residual deformation to be smaller. For stress relaxation studies there are no standard specifications about test parameters, and therefore it is difficult to make a compar-ison with other studies. However, the viscoelastic response of SFt/gel structures is similar to that found for other vas-cular grafts and typical of physiological arteries [54].

SFt and SFt/gel structures demonstrated very good in vitro cytocompatibility, in accordance with previous studies focusing on in vitro interactions of different cell types with ES-SF [1, 2, 9]. Despite the low difference observed in vitro, gelatin coating still remains an important feature for successful graft application, as it can act as a sealant for the first stages after implantation and also induces low platelet adhesion [28].

5 Conclusion

The innovative method evaluated here for coating ES-SF tubular scaffold with crosslinked gelatin gel, appears as an effective strategy to overcome the several limitations encountered by standard small diameter blood vessel grafts. To the best of the authors' knowledge, gelatin gel has never been used as coating of small diameter vascular grafts before. Due to its biocompatibility, gelatin is used as sealant of large caliber synthetic vascular prostheses, where it has demonstrated to improve cell interaction [55]. Compared to other natural proteins (i.e. collagen, elastin, fibrin, fibronectin) investigated as coating for decellularized or syn-thetic vascular grafts to improve their cytocompatibility [45, 56, 57] or to decrease platelet adhesion (elastin, fibrin) [58–60] gelatin not only possesses excellent cytocompatibility, but it also causes low platelet adhesion. Furthermore, gelatin is less expensive than all the other biomolecules and more easily available.

The crosslinking method developed overcomes gelatin limited stability at 37 °C, as the gel coating proved to be stable up to 13 days while maintaining good cell compatibility, which is therefore not significantly affected by the crosslinking reaction. In addition, for the first time, a gelatin coating has been used on a natural polymer vascular graft. The use of SF for graft structure allows to overcome many problems related to both decellularized matrices (i.e. thrombosis, calcification and immune response against donor cell remnants) [57] and synthetic polymers (i.e. thrombosis and anastomotic intimal hyperplasia) [58–61] in small caliber vessel replacement or regeneration. Electro-spun fibroin grafts have already demonstrated excellent properties for vascular regeneration in an in vivo study [10]. The innovative SFt/gel structure developed in this work not only demonstrated adequate morphological properties (to support cell colonization), but also suitable structure degradation kinetics, and burst pressure and mechanical compliance close to saphenous and umbilical veins, the gold standard for small caliber vascular replacement. The per se remarkable biocompatibility of SF is here combined with a coating that acts as a sealant and is capable to pro-mote cell adhesion and proliferation in the first days after implantation and, most of all, induces low platelet adhesion,

which both are critical issues in early stages of vascular regeneration. Hence, the SFt/gel structure represents a promising alternative to overcome the current graft drawbacks and obtain a vascular graft with adequate stability as well as morphological, mechanical and biological properties for in vivo tissue engineering of small diameter blood vessel.

Conflict of interest The authors declare that they have no competing interests.

References

1. Catto V, Fare S, Cattaneo I, Figliuzzi M, Alessandrino A, Freddi G, Remuzzi A, Tanzi MC. Small diameter electrospun silk fibroin vascular grafts: mechanical properties, in vitro biodegradability, and in vivo biocompatibility. Mater Sci Eng C. 2015;54:101–11.
2. Marelli B, Alessandrino A, Fare S, Freddi G, Mantovani D, Tanzi MC. Compliant electrospun silk fibroin tubes for small vessel bypass grafting. Acta Biomater. 2010;6:4019–26.
3. Rathore A, Cleary M, Naito Y, Rocco K, Breuer C. Development of tissue engineered vascular grafts and application of nanomedicine. Wires Nanomed Nanobiotechnol. 2012;4:257–72.
4. Catto V, Fare S, Freddi G, Tanzi MC. Vascular tissue engineering: recent advances in small diameter blood vessel regeneration. ISRN Vasc Med. 2014;2014:27
5. Zhang XH, Baughman CB, Kaplan DL. In vitro evaluation of electrospun silk fibroin scaffolds for vascular cell growth. Biomaterials. 2008;29:2217–27.
6. Lovett M, Eng G, Kluge JA, Cannizzaro C, Vunjak-Novakovic G, Kaplan DL. Tubular silk scaffolds for small diameter vascular grafts. Organogenesis. 2010;6:217–24.
7. Wang SD, Zhang YZ, Wang HW, Yin GB, Dong ZH. Fabrication and properties of the electrospun polylactide/silk fibroin-gelatin composite tubular scaffold. Biomacromolecules. 2009;10: 2240–44.
8. Pankajakshan D, Agrawal DK. Scaffolds in tissue engineering of blood vessels. Can J Physiol Pharm. 2010;88:855–73.
9. Marelli B, Achilli M, Alessandrino A, Freddi G, Tanzi MC, Fare S, Mantovani D. Collagen-reinforced electrospun silk fibroin tubular construct as small calibre vascular graft. Macromol Biosci. 2012;12:1566–74.
10. Cattaneo I, Figliuzzi M, Azzollini N, Catto V, Fare S, Tanzi MC, Alessandrino A, Freddi G, Remuzzi A. In vivo regeneration of elastic lamina on fibroin biodegradable vascular scaffold. Int J Artif Organs. 2013;36:166–74.
11. Lee KY, Mooney DJ. Hydrogels for tissue engineering. Chem Rev. 2001;101:1869–79.
12. Hoch E, Schuh C, Hirth T, Tovar GEM, Borchers K. Stiff gelatin hydrogels can be photo-chemically synthesized from low viscous gelatin solutions using molecularly functionalized gelatin with a high degree of methacrylation. J Mater Sci. 2012;23:2607–17.
13. Young S, Wong M, Tabata Y, Mikos AG. Gelatin as a delivery vehicle for the controlled release of bioactive molecules. J Control Release. 2005;109:256–74.
14. Altman GH, Diaz F, Jakuba C, Calabro T, Horan RL, Chen JS, Lu H, Richmond J, Kaplan DL. Silk-based biomaterials. Biomaterials. 2003;24:401–16.
15. Wray LS, Hu X, Gallego J, Georgakoudi I, Omenetto FG, Schmidt D, Kaplan DL. Effect of processing on silk-based biomaterials: reproducibility and biocompatibility. J Biomed Mater Res B. 2011;99B:89–101.
16. Rockwood DN, Preda RC, Yucel T, Wang XQ, Lovett ML, Kaplan DL. Materials fabrication from Bombyx mori silk fibroin. Nat Protoc. 2011;6:1612–31.
17. Motta A, Migliaresi C, Faccioni F, Torricelli P, Fini M, Giardino R. Fibroin hydrogels for biomedical applications: preparation, characterization and in vitro cell culture studies. J Biomater Sci Polym Ed. 2004;15:851–64.
18. Sugihara A, Sugiura K, Morita H, Ninagawa T, Tubouchi K, Tobe R, Izumiya M, Horio T, Abraham NG, Ikehara S. Promotive effects of a silk film on epidermal recovery from full-thickness skin wounds. Proc Soc Exp Biol Med. 2000;225:58–64.
19. Meinel L, Hofmann S, Karageorgiou V, Zichner L, Langer R, Kaplan D, Vunjak-Novakovic G. Engineering cartilage-like tissue using human mesenchymal stem cells and silk protein scaffolds. Biotechnol Bioeng. 2004;88:379–91.
20. Yeo JH, Lee KG, Kim HC, Oh YL, Kim AJ, Kim SY. The effects of PVA/Chitosan/Fibroin (PCF)-blended spongy sheets on wound healing in rats. Biol Pharm Bull. 2000;23:1220–23.
21. Fischer RL, McCoy MG, Grant SA. Electrospinning collagen and hyaluronic acid nanofiber meshes. J Mater Sci. 2012;23:1645–54.
22. Soffer L, Wang XY, Zhang XH, Kluge J, Dorfmann L, Kaplan DL, Leisk G. Silk-based electrospun tubular scaffolds for tissue-engineered vascular grafts. J Biomater Sci Polym Ed. 2008;19: 653–664.
23. Salacinski HJ, Goldner S, Giudiceandrea A, Hamilton G, Seifalian AM, Edwards A, Carson RJ. The mechanical behavior of vascular grafts: a review. J Biomater Appl. 2001;15:241–78.
24. Kannan RY, Salacinski HJ, Butler PE, Hamilton G, Seifalian AM. Current status of prosthetic bypass grafts: a review. J Biomed Mater Res B. 2005;74B:570–81.
25. Mizelle S. W., Gupta B. S., Kasyanov V. A. (1995) Compliance of small-diameter vascular grafts as a determinant of patency. Proceedings of the 1995 Fourteenth Southern Biomedical Engineering Conference 1995. 7–9 April 1995, pp. 30–33.
26. Konig G, McAllister TN, Dusserre N, Garrido SA, Iyican C, Marini A, Fiorillo A, Avila H, Wystrychowski W, Zagalski K, Maruszewski M, Jones AL, Cierpka L, de la Fuente LM, L'Heureux N. Mechanical properties of completely autologous human tissue engineered blood vessels compared to human saphenous vein and mammary artery. Biomaterials. 2009; 30:1542–50.
27. Enomoto S, Sumi M, Kajimoto K, Nakazawa Y, Takahashi R, Takabayashi C, Asakura T, Sata M. Long-term patency of small-diameter vascular graft made from fibroin, a silk-based biodegradable material. J Vasc Surg. 2010;51:155–64.
28. Siess W. Molecular mechanism of platelet activation. Fortschr Med. 1985;103:937
29. Madaghiele M, Piccinno A, Saponaro M, Maffezzoli A, Sannino A. Collagen- and gelatine-based films sealing vascular prostheses: evaluation of the degree of crosslinking for optimal blood impermeability. J Mater Sci. 2009;20:1979–89.
30. Kretlow JD, Klouda L, Mikos AG. Injectable matrices and scaffolds for drug delivery in tissue engineering. Adv Drug Deliv Rev. 2007;59:263–73.
31. Kuijpers AJ, Engbers GHM, Krijgsveld J, Zaat SAJ, Dankert J, Feijen J. Cross-linking and characterisation of gelatin matrices for biomedical applications. J Biomater Sci Polym Ed. 2000;11:225–43.
32. Wang SD, Zhang YZ, Yin GB, Wang HW, Dong ZH. Fabrication of a composite vascular scaffold using electrospinning technology. Mater Sci Eng C. 2010;30:670–76.
33. Okhawilai M, Rangkupan R, Kanokpanont S, Damrongsakkul S. Preparation of Thai silk fibroin/gelatin electrospun fiber mats for controlled release applications. Int J Biol Macromol. 2010;46:544–50.
34. Somvipart S, Kanokpanont S, Rangkupan R, Ratanavaraporn J, Damrongsakkul S. Development of electrospun beaded fibers

from Thai silk fibroin and gelatin for controlled release application. Int J Biol Macromol. 2013;55:176–84.
35. Gui-bo Y, You-zhu Z, Wei-wei B, Jialin W, De-bing S, Zhi-hui D, Wei-guo F. Study on the properties of the electrospun silk fibroin/gelatin blend nanofibers for scaffolds. J Appl Polym Sci. 2009;111:1471–77.
36. Tanzi MC, Fare' S, Gerges I. Crosslinked gelatin hydrogels. PCT/EP2012/060277. 2012
37. Achilli M, Meghezi S, Mantovani D. On the viscoelastic properties of collagen-gel-based lattices under cyclic loading: applications for vascular tissue engineering. Macromol Mater Eng. 2012;297:724–34.
38. Sato M, Nakazawa Y, Takahashi R, Tanaka K, Sata M, Aytemiz D, Asakura T. Small-diameter vascular grafts of Bombyx mori silk fibroin prepared by a combination of electrospinning and sponge coating. Mater Lett. 2010;64:1786–88.
39. Chen KY, Dong GC, Hsu CY, Chen YS, Yao CH. Autologous bone marrow stromal cells loaded onto porous gelatin scaffolds containing Drynaria fortunei extract for bone repair. J Biomed Mater Res A. 2013;101:954–62.
40. Liang HC, Chang WH, Liang HF, Lee MH, Sung HW. Crosslinking structures of gelatin hydrogels crosslinked with genipin or a water-soluble carbodiimide. J Appl Polym Sci. 2004;91:4017–26.
41. Yao L, Liu JY, Andreadis ST. Composite fibrin scaffolds increase mechanical strength and preserve contractility of tissue engineered blood vessels. Pharm Res. 2008;25:1212–21.
42. McKenna KA, Hinds MT, Sarao RC, Wu PC, Maslen CL, Glanville RW, Babcock D, Gregory KW. Mechanical property characterization of electrospun recombinant human tropoelastin for vascular graft biomaterials. Acta Biomater. 2012;8:225–33.
43. Tillman BW, Yazdani SK, Lee SJ, Geary RL, Atala A, Yoo JJ. The in vivo stability of electrospun polycaprolactone-collagen scaffolds in vascular reconstruction. Biomaterials. 2009;30:583–588.
44. Wu W, Allen RA, Wang YD. Fast-degrading elastomer enables rapid remodeling of a cell-free synthetic graft into a neoartery. Nat Med. 2012;18:1148
45. He W, Ma ZW, Teo WE, Dong YX, Robless PA, Lim TC, Ramakrishna S. Tubular nanofiber scaffolds for tissue engineered small-diameter vascular grafts. J Biomed Mater Res A. 2009;90A:205–16.
46. Uchida T, Ikeda S, Oura H, Tada M, Nakano T, Fukuda T, Matsuda T, Negoro M, Arai F. Development of biodegradable scaffolds based on patient-specific arterial configuration. J Biotechnol. 2008;133:213–18.
47. Wise SG, Byrom MJ, Waterhouse A, Bannon PG, Weiss AS, Ng MKC. A multilayered synthetic human elastin/polycaprolactone hybrid vascular graft with tailored mechanical properties. Acta Biomater. 2011;7:1429
48. Wang C, Cen L, Yin S, Liu QH, Liu W, Cao YL, Cui L. A small diameter elastic blood vessel wall prepared under pulsatile conditions from polyglycolic acid mesh and smooth muscle cells differentiated from adipose-derived stem cells. Biomaterials. 2010;31:621–30.
49. de Valence S, Tille JC, Giliberto JP, Mrowczynski W, Gurny R, Walpoth BH, Moller M. Advantages of bilayered vascular grafts for surgical applicability and tissue regeneration. Acta Biomater. 2012;8:3914–20.
50. de Valence S, Tille JC, Mugnai D, Mrowczynski W, Gurny R, Moller M, Walpoth BH. Long term performance of polycaprolactone vascular grafts in a rat abdominal aorta replacement model. Biomaterials. 2012;33:38–47.
51. Roh JD, Nelson GN, Brennan MP, Mirensky TL, Yi T, Hazlett TF, Tellides G, Sinusas AJ, Pober JS, Saltzman WM, Kyriakides TR, Breuer CK. Small-diameter biodegradable scaffolds for functional vascular tissue engineering in the mouse model. Biomaterials. 2008;29:1454–63.
52. McClure MJ, Sell SA, Simpson DG, Walpoth BH, Bowlin GL. A three-layered electrospun matrix to mimic native arterial architecture using polycaprolactone, elastin, and collagen: a preliminary study. Acta Biomater. 2010;6:2422–33.
53. Lee SJ, Liu J, Oh SH, Soker S, Atala A, Yoo JJ. Development of a composite vascular scaffolding system that withstands physiological vascular conditions. Biomaterials. 2008;29:2891–98.
54. Berglund JD, Nerem RM, Sambanis A. Viscoelastic testing methodologies for tissue engineered blood vessels. J Biomech Eng. 2005;127:1176–84.
55. Manju S, Muraleedharan CV, Rajeev A, Jayakrishnan A, Joseph R. Evaluation of alginate dialdehyde cross-linked gelatin hydrogel as a biodegradable sealant for polyester vascular graft. J Biomed Mater Res B. 2011;98B:139–49.
56. Lu WD, Zhang M, Wu ZS, Hu TH. Decellularized and photo-oxidatively crosslinked bovine jugular veins as potential tissue engineering scaffolds. Interact Cardiovasc Thorac Surg. 2009;8:301–5.
57. Assmann A, Delfs C, Munakata H, Schiffer F, Horstkotter K, Huynh K, Barth M, Stoldt VR, Kamiya H, Boeken U, Lichtenberg A, Akhyari P. Acceleration of autologous in vivo recellularization of decellularized aortic conduits by fibronectin surface coating. Biomaterials. 2013;34:6015–26.
58. Jordan SW, Haller CA, Sallach RE, Apkarian RP, Hanson SR, Chaikof EL. The effect of a recombinant elastin-mimetic coating of an ePTFE prosthesis on acute thrombogenicity in a baboon arteriovenous shunt. Biomaterials. 2007;28:1191–97.
59. Koch S, Flanagan TC, Sachweh JS, Tanios F, Schnoering H, Deichmann T, Ella V, Kellomaki M, Gronloh N, Gries T, Tolba R, Schmitz-Rode T, Jockenhoevel S. Fibrin-polylactide-based tissue-engineered vascular graft in the arterial circulation. Biomaterials. 2010;31:4731–39.
60. Deutsch M, Meinhart J, Zilla P, Howanietz N, Gorlitzer M, Froeschl A, Stuempflen A, Bezuidenhout D, Grabenwoeger M. Long-term experience in autologous in vitro endothelialization of infrainguinal ePTFE grafts. J Vasc Surg. 2009;49:352–62.
61. Woodhouse KA, Klement P, Chen V, Gorbet MB, Keeley FW, Stahl R, Fromstein JD, Bellingham CM. Investigation of recombinant human elastin polypeptides as non-thrombogenic coatings. Biomaterials. 2004;25:4543–53.